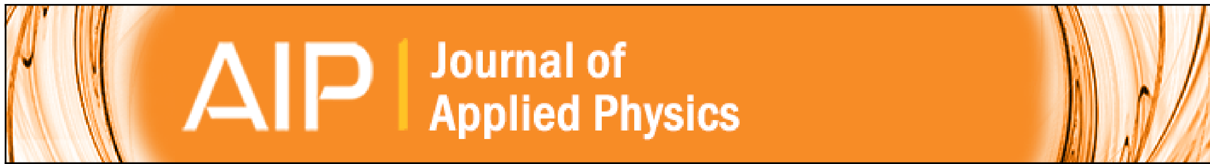

A direct measurement of the electronic structure of Si nanocrystals and its effect on optoelectronic properties

Waqas Mustafeez, Arka Majumdar, Jelena Vukovi, and Alberto Salleo

Citation: Journal of Applied Physics **115**, 103515 (2014); doi: 10.1063/1.4868299
View online: http://dx.doi.org/10.1063/1.4868299
View Table of Contents: http://scitation.aip.org/content/aip/journal/jap/115/10?ver=pdfcov
Published by the AIP Publishing

Re-register for Table of Content Alerts

Create a profile.

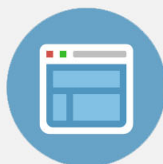

Sign up today!

[This article is copyrighted as indicated in the article. Reuse of AIP content is subject to the terms at: http://scitation.aip.org/termsconditions. Downloaded to] IP: 171.67.216.22 On: Mon, 17 Mar 2014 23:00:43

JOURNAL OF APPLIED PHYSICS **115**, 103515 (2014)

A direct measurement of the electronic structure of Si nanocrystals and its effect on optoelectronic properties

Waqas Mustafeez,[1] Arka Majumdar,[2] Jelena Vučković,[2] and Alberto Salleo[1,a)]
[1]*Geballe Laboratory for Advanced Materials, Stanford University, Stanford, California 94305, USA*
[2]*Ginzton Laboratory, Stanford University, California 94305, USA*

(Received 7 February 2014; accepted 28 February 2014; published online 13 March 2014)

Since reports that silicon nanocrystals (Si-NCs) can exhibit direct transition emission, the silicon laser field is at a juncture where the importance of this discovery needs to be evaluated. Most theoretical models predicted a monotonic increase in the bandgap and experimental information currently available on the electronic structure at the Γ valley of these promising materials is circumstantial as it is obtained from emission measurements where competing non-radiative relaxation and recombination processes only provide an incomplete picture of the electronic structure of Si-NCs. Optical absorption, the most immediate probe of the electronic structure beyond the band-edges, showing the evolution of the Γ valley states with nanocrystal size has not been measured. Here, we show such measurements, performed with high dynamic range, allowing us to observe directly the effect of crystal size on the Γ valley splitting far above the band-edges. We show that the splitting is 100 s of meV more pronounced than predicted by pseudo potential calculations and Luttinger-Kohn model. We also show that ultrafast red-shifting emission can be observed in plasma enhanced chemical vapor deposition prepared Si-NCs. © *2014 AIP Publishing LLC*. [http://dx.doi.org/10.1063/1.4868299]

I. INTRODUCTION

The first report of single pass or transient gain in Si-NCs in 2000 generated much excitement.[1] Within this context, the synthesis and optoelectronic properties of Si-NCs have been extensively studied.[2–5] Using quantum confinement effects in Si-NCs with size between 2 and 6 nm, it is possible to tune light emission due to indirect recombination in the 700 to 1000 nm range. Optical gain, however, is fundamentally limited by the free carrier absorption (FCA) cross-section of the nanocrystals, which increases due to small size effects.[6,7] Indeed, as soon as pump power is increased in a multi-pass design, such as in a resonant cavity, FCA starts to dominate. The FCA-associated loss is approximately of the same order of magnitude as the gain from these crystals thereby suppressing the ability of the cavity to lase.[8]

One strategy proposed in recent years to achieve multi-pass gain has been to focus on the F (fast) direct band recombination in Si-NC, as opposed to the S (slow) band associated with phonon-assisted excitonic recombination.[9,10] The F-band emission is promising because the emission rate is fast and comparable to direct transition materials and the coupling with a nanophotonic cavity improves when temperatures are lowered. The higher photon energy operation also offers reduced free carrier absorption losses. It should be noted that while blue emission can also be obtained from Si-NCs synthesized via colloidal routes, these are currently not suitable for solid state laser sources as their incorporation into nanophotonic structures is much more challenging.[11]

The origins of the F-band have been debated, with many reports pointing to a size-independent emissive defect with decay time scales on the order of ns.[12] Other reports, however, proved that the F-band actually consists of a ps core-related component in addition to ns decay from defects.[13] Understanding the band structure of Si-NCs at high energy and the decay channels giving rise to the F-band is clearly extremely relevant to determining whether multi-pass gain can indeed be obtained in these materials. While there are many discordant theoretical predictions of the effects of quantum confinement on the higher energy levels in Si-NCs in an oxide matrix, there is currently no direct experimental measurement of these effects.

In contrast with the well-known behavior of the S-band, which is associated with indirect recombination, quantum confinement leads to a red-shift with decreasing crystal size of the F-band. The F-band is observable at the ∼100 s of ps timescale (Fig. 1). This shift excludes defect-based processes as a possible origin of the emission. Hence, the F-band in high quality Si-NCs is purported to originate from the direct recombination of negative effective-mass states at the Γ valley. Using pseudo-potential calculations, the quantum-confinement induced red-shift of the direct recombination energy was initially reported as an anomaly and to be on the order of 100 meV even down to 2 nm crystal sizes.[14] At the time most calculations of the full band structure predicted an increase in the direct gap as NC size was reduced. Some later works, however, do show that in reality some of the Γ states decrease in energy while others increase, thus causing a split within the conduction band.[15,16] The purpose of this work is to measure the direct bandgap of Si nanoparticles and its dependence on particle size using optical absorption, rather than emission as previously done.

II. EXPERIMENTAL METHODS

For this study, we prepared Si-NCs in a solid SiO_2 matrix by fabricating silicon-rich oxide (SRO) films using plasma enhanced chemical vapor deposition (PECVD).

[a)]asalleo@stanford.edu

 © 2014 AIP Publishing LLC

[This article is copyrighted as indicated in the article. Reuse of AIP content is subject to the terms at: http://scitation.aip.org/termsconditions. Downloaded to] IP: 171.67.216.22 On: Mon, 17 Mar 2014 23:00:43

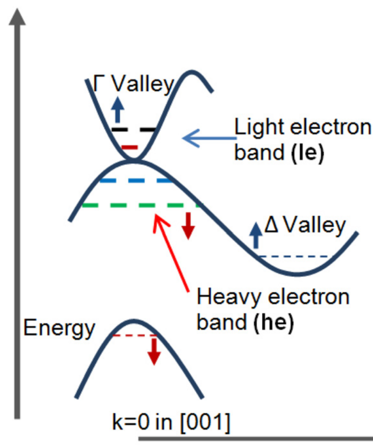

FIG. 1. Illustration of the E(k) diagram of silicon nanocrystals and the splitting mechanism due to opposite signs of the electron effective mass in the conduction band at the Γ(k = 0) point.

PECVD deposition was performed at 350 °C with an rf generator set at 13.56 MHz. The flow rate of SiH_4 to N_2O was varied to control the overall composition of SiO_x. Deposition was followed by 1-h anneals in the 900 °C to 1140 °C range in an N_2 atmosphere to precipitate the crystals and by 1-h forming gas passivation at 400 °C to reduce surface dangling bond based defects. The final film thickness was measured using spectroscopic ellipsometry to be approximately 500 nm. The resultant films contained about 8% by atomic weight nitrogen. In order to produce the best results to date in terms of internal quantum efficiency and overall performance, Si-NCs must be encapsulated in SiO_2, which also minimizes spurious interface recombination.[17] It should be added that, until now, efficient F-band emission was observed only in high-quality Si-NCs prepared by RF co-sputtering. We show that PECVD can be used to prepare equally high-quality Si-NCs (*vide infra*). From the manufacturing prospective, PECVD is advantageous compared to RF-co-sputtering because it can afford much larger throughput.

PL has regularly been used to study the electronic properties of these systems; however, emission measurements involve the relaxation process through radiative and non-radiative processes and thus do not provide a complete picture of band structure evolution. As a result, we directly measure band-to-band absorption in our films using photothermal deflection spectroscopy (PDS), a high-dynamic-range optical absorption measurement technique in the 1 eV to 4 eV range (i.e., above the bandgap).[18] Briefly, PDS measures the heat released by the non-radiative relaxation following the optical excitation of the film caused by a monochromated temporally modulated pump beam. The heat causes the deflection of a laser beam grazing the surface of the sample, which is immersed in a liquid (mirage effect). Locking-in the deflection to the pump modulation allows us to achieve high sensitivity. We used a chopped halogen lamp source incident onto the NCs through a monochromator with the deflected laser signal collected through a lock-in amplifier with a 10 s integration time at each pump wavelength. The inert immersion fluid used was commercial fluorinert FC-72.

III. EXPERIMENTAL RESULTS

The unnormalized PDS spectra are shown in Figure 2. In order to make quantitative comparisons and calculate the absorption cross section, the spectra need to be normalized. We obtain the average size and the relative concentration of Si nanocrystals of the annealed films integrating the x-ray diffraction (XRD) signal from the [311] peak shown in Figure 2(b). This procedure allows us to normalize to the amount of crystalline material in each film. In order to calculate the absorption cross section, we used XPS to calculate

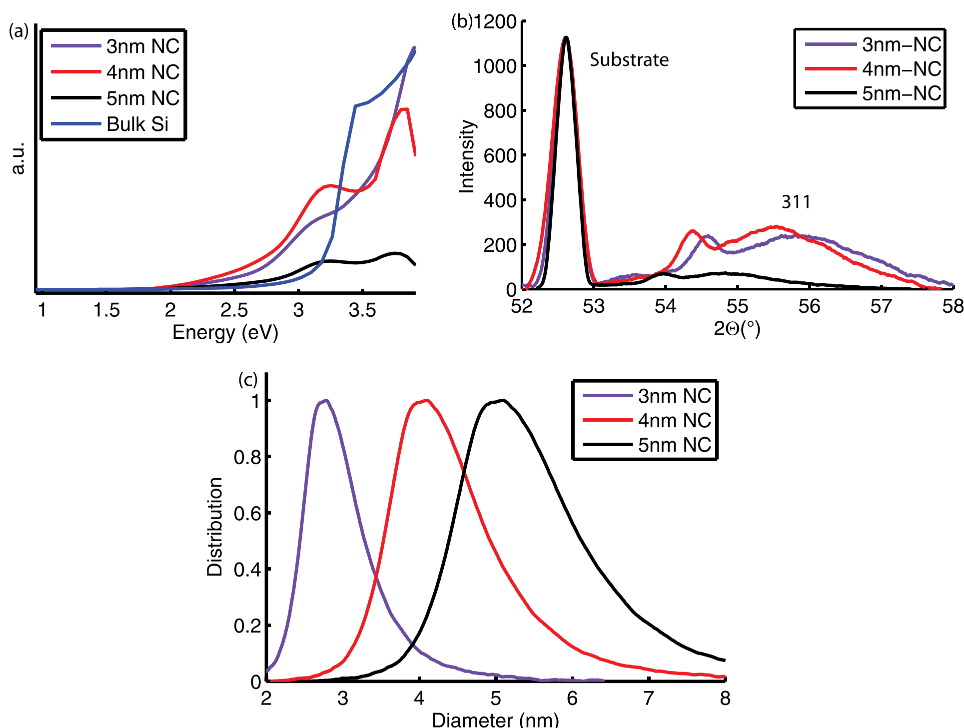

FIG. 2. (a) PDS curve before normalization and calibration. XRD in (b) shows the relative crystallinity of the films from the 311 peak. The film with 5 nm crystals had four times lower crystallinity than the 3 and 4 nm films. (c) The size distribution for the three films obtained using the analytical model in Ref. 21. The films with smaller average crystal sizes also have smaller distributions, 20%, 32%, and 34%, respectively, for 3 nm, 4 nm, and 5 nm films.

[This article is copyrighted as indicated in the article. Reuse of AIP content is subject to the terms at: http://scitation.aip.org/termsconditions. Downloaded to] IP: 171.67.216.22 On: Mon, 17 Mar 2014 23:00:43

the excess silicon in each film. Under the assumption that all excess Si crystallized after annealing, silicon nanocrystals per unit volume (N_{nc}) can then be calculated from the geometry and excess c-Si content (Si_p) of the film using

$$N_{nc} = \frac{Si_p}{\frac{4}{3}\pi r^3}\,\mathrm{cm}^{-3}. \quad (1)$$

Then, the nanocrystal cross section (σ_{nc}) can be calculated from the absorption coefficient (σ) using

$$\sigma_{nc} = \frac{\sigma}{N_{nc}}\,\mathrm{cm}^2. \quad (2)$$

In order to reliably use the absorption results, we must ensure that the Si-NC size distribution is limited. The relationship between the NC size and emission energy has been established via high-resolution transmission electron microscopy studies.[19] Under the assumption that the probability of emission is independent of crystal size, we get the analytical expression relating TEM obtained size distribution and PL linewidths.

$$D(E) = \left(\frac{1.86}{E - E_{bulk}}\right)^{\frac{1}{1.39}}, \quad (3)$$

where D is diameter, E is emission, and E_{bulk} is the bandgap of bulk Si. For our samples, the distribution width ranges from 20% to 34% and is state of the art.[21]

Our PDS setup is sensitive down to 10^{-4} changes in absorption over a span of 5 orders of magnitude and is thus able to resolve very small changes in the optical properties of the film due to quantum confinement in Si-NCs, even though these changes occur on top of a strong background signal due to the increasing Si-NC and matrix absorption at high energies. Furthermore, due to the nature of the excitation and detection mechanism, PDS is largely insensitive to artifacts caused by scattering or emission, especially in poor emitters like Si-NCs. We found that some of the high energy features in optical absorption measurements in Si-NCs were beyond the dynamic range of other conventional techniques such as ellipsometry and UV-VIS absorption spectroscopy. Our results thus provide previously unattainable experimental information about the electronic structure at the Γ_{15} point of thermally grown Si-NCs embedded in an oxide matrix.[8] By overlapping the PDS spectra with conventional UV-Visible spectroscopy in a limited spectral range and by using the XRD data to estimate the volume density of Si-NCs, we obtain the absorption cross section for the three sizes (Fig. 3(a)). At the onset of the indirect absorption, i.e., 1.7 eV, 1.51 eV, and 1.4 eV, the absorption cross-section is 1.6×10^{-16} cm^2, 1.12×10^{-16} cm^2, and 8.6×10^{-17} cm^2 for crystals of diameter 3, 4, and 5 nm, respectively, and matches previous reports (Figs. 3(a) and 3(b)).[20] The variation in absorption cross section is an interplay between the oscillator strength (OS), FCA, and density of states (DOS). The higher OS and FCA in smaller crystals cause an increase in the absorption cross section despite lower DOS. The onset of the absorption edge corresponds perfectly to the peak emission energy of the S-band, confirming that it originates from the indirect transition.

The high-energy part of the absorption spectra of the Si-NCs can be generally described as having two peaks instead of the single feature present in bulk Si, a hallmark of the artificial atom nature of the NCs. The exact positions of the peaks depend on crystal size. Comparing the Si-NC spectra to bulk Si absorption allows us to assign these spectral features to the Γ_{15} point. The two peaks are caused by the splitting of the heavy electron (he), light electron (le), and mixed (me) states with quantum confinement. With decreasing crystal size, the heavy electron states shift higher in energy, the light electron states shift lower in energy, while the mixed states move either higher or lower depending on the quantum number. The opposing motion of these three transitions results in a DOS minimum at 3.4 eV (Fig. 3(c)).

The evolution of absorption cross-section of Si-NCs with size provides experimental proof supporting the F-band red shift as some of the heavy electron and mixed states move down in energy with confinement. In addition, it also allows validation of various theoretical models that predicted such a shift. At the Γ valley, one band has a positive effective mass and the other one has a negative effective mass (Fig. 1). The energy of the quasi-particles with positive effective mass increases when the crystal size is reduced. Hence, a blue-shift of the indirect transition (~1.7 eV from 1.12 eV for 3 nm NCs) is observed. Similarly, the positive effective mass states and some mixed positive-negative states cause a blue-shift of the higher-energy component of the direct transition (~3.7 eV from 3.5 eV for 3 nm NCs). The energy of negative effective-mass and some mixed states on the other hand decreases in smaller crystals. The lowest quantum number red-shifting states at the direct transition ($1he_0$ to $1mh_2$) involve mixed holes and negative effective mass electrons. Thus, the overall effect of quantum confinement is a decrease in the absorption energy and splitting of the conduction band.

We compare the shift observed with two theoretical studies that simulated shifts with crystal size in the lowest order states at the Γ point states. Krishna *et al.*[15] were the first group to predict a redshift in Si-NCs energy levels using pseudopotential calculations. Prokofiev *et al.*[21] studied the same energy levels using the Luttinger-Kohn model. Both of these theoretical results are compared in Figure 3(c). The results from Krishna *et al.* showed no definitive splitting until a crystal diameter of 2 nm. The Luttinger-Kohn model provides a reasonable approximation but still underestimates the shift by 100 s of meV. The sign of the effective mass only provides a first-order approximation, various states in the band have a combined effect on the movement of any single state as captured by the Luttinger-Kohn model. Our optical absorption measurements allow us to estimate experimentally the quantum-confinement-induced splitting of the conduction band at the Γ point, which for 3-nm nanoparticles is ~870 meV (Fig. 3(c)). Finite particle size distribution, the relative proximity of the split energy levels in combination with the high measurement temperature (298 K) all contribute to the broadening of the absorption features thus individual states cannot be observed. The size-dependence trends and the order of magnitude of the

[This article is copyrighted as indicated in the article. Reuse of AIP content is subject to the terms at: http://scitation.aip.org/termsconditions. Downloaded to] IP: 171.67.216.22 On: Mon, 17 Mar 2014 23:00:43

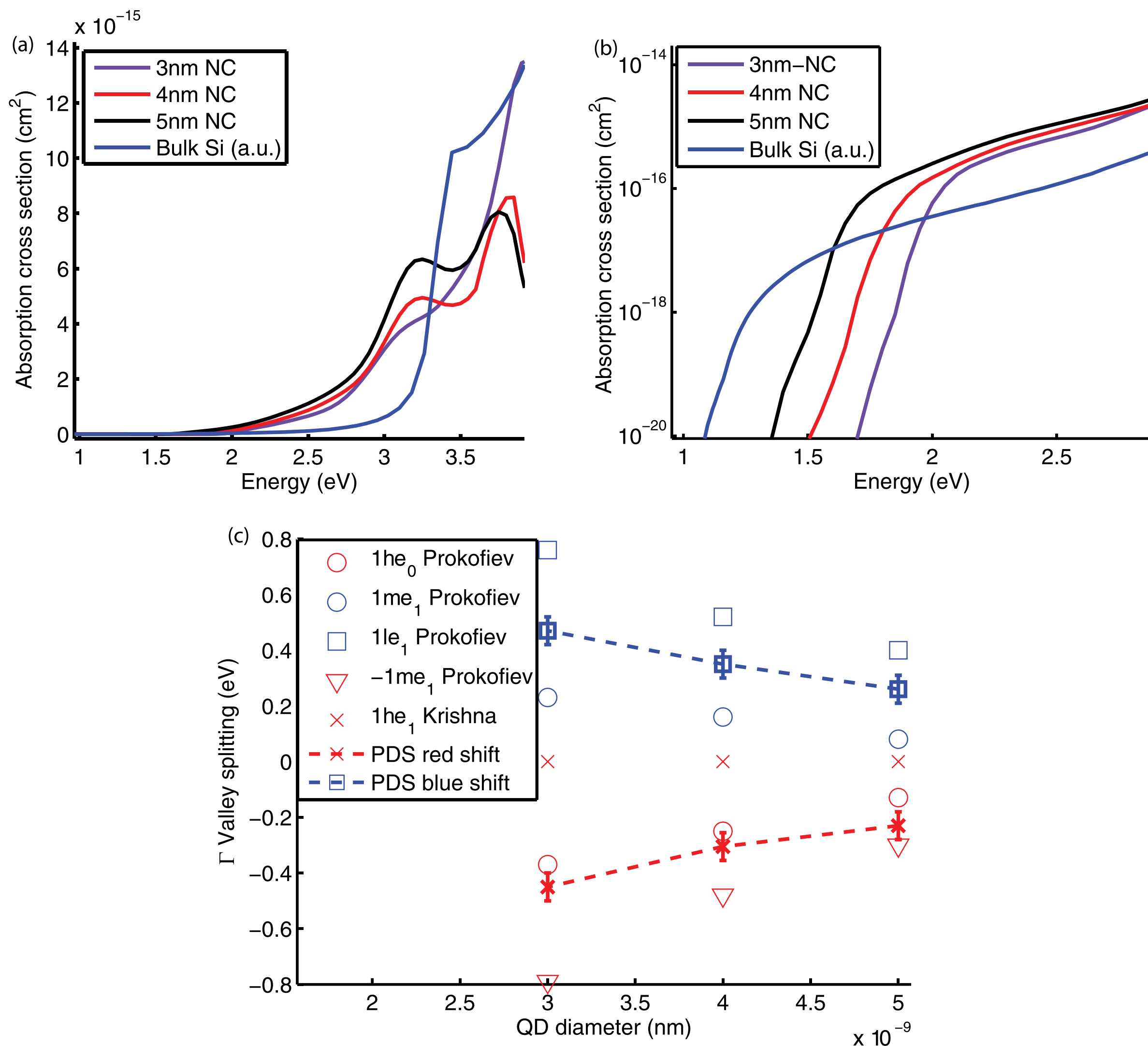

FIG. 3. (a) Absorption cross section spectra for the three quantum dot sizes. Bulk silicon absorption is in arbitrary units. The onset of the direct transition leads to a sharp increase in absorption in bulk material at 3.4 eV. However, in the Si-NCs this feature is split into two features leaving an absorption minimum in-between. The arrows highlight the center of the Lorentzian fit for the splitting of the conduction band. The low energy part of the spectrum shows the effect of quantum confinement on the absorption onset and is displayed on a log scale in (b) to demonstrate that the absorption onset energy corresponds to the S-band emission energy (Fig. 2). Comparison of the splitting observed with pseudopotential and Luttinger-Kohn models (c), in particular, we display the lowest order heavy electron (he), light electron (le), and mixed states (me). The number preceding the state name is the quantum number "n" and the subscript is the total angular momentum "F."

energy splitting predicted by Prokofiev *et al*. are in agreement with our experimental measurements; however, the lack of a quantitative agreement highlights the need for further theoretical developments.

IV. EMISSION CHARACTERISTICS

In order to confirm that the electronic structure we measured by PDS is responsible for the emission behavior of the Si-NCs, we discuss the time-resolved PL (Fig. 4). For the ps decay measurement, we used a 380 nm (3.26 eV), approximately 30 ps pulsed laser with a repetition rate of 80 MHz. The resulting PL was dispersed by a grating with a 2-nm spectral resolution, and sent to single photon counters (Hamamatsu). The temporal dynamics was obtained by measuring the photon arrivals with a Pico-Harp picosecond time analyzer, where the time-origin was determined by the laser pulse. The μs decay was measured using a 532 nm, 12 ns pulsed laser (10 Hz repetition rate) and an avalanche photodiode.

We can separate direct band and indirect band emissions by taking advantage of their different timescales. Shifts up to 1100 meV (from 3.2 eV to 2 eV for crystal sizes decreasing from 5.5 nm to 2.5 nm) were observed in the strongest emitting Γ transition.[22] Emission from all three samples exhibits a fast ps decay of 410 ps, 500 ps, and 620 ps (F-band) for 3 nm, 4 nm, and 5 nm crystals, respectively. In addition, there is a ~50 ns decay and a μs decay (S-band). As expected, emission from the F-band is strongly suppressed at lower energy (<1.5 eV), which is consistent with it being caused by a higher-energy direct transition (Fig. 4). The ultrafast decay rate of the direct transition, limited by the transition time from the Γ point to the X point would imply an ultrafast rise time of indirect emission. This rise time is known to be

[This article is copyrighted as indicated in the article. Reuse of AIP content is subject to the terms at: http://scitation.aip.org/termsconditions. Downloaded to] IP: 171.67.216.22 On: Mon, 17 Mar 2014 23:00:43

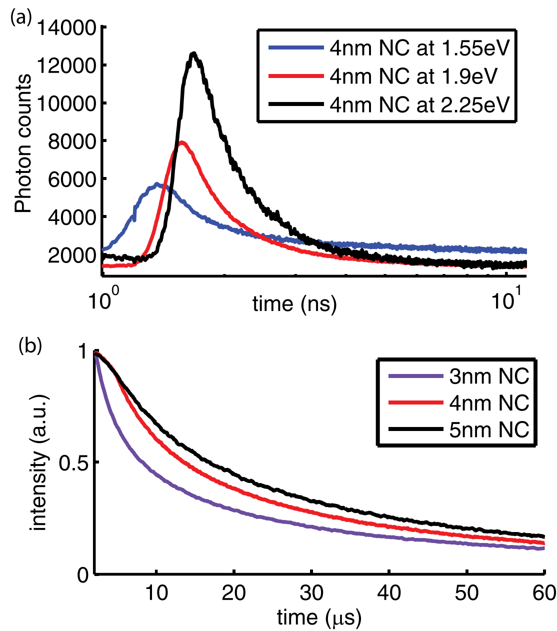

FIG. 4. (a) The temporal decay of the PL shows a ns component due to defects and a faster ps decay component corresponding to the F-band. The efficiency of the decay varies with excitation energy. Slower μs decay of the peak PL due to indirect recombination from states in the Δ valley (measured at 1.5 eV, 1.58 eV, and 1.7 eV) of samples with 5 nm, 4 nm, and 3 nm NCs (b). Phonon assisted recombination becomes more efficient as the crystal diameter decreases causing a faster PL decay.

sub-ns and thus is consistent with our results.[23] The observed ~50 ns-decay on the other hand is known to vary based on passivation through a forming gas anneal (from a few ns to several tens of nanoseconds). The dependence of the decay time on passivation is consistent with non-radiative recombination at defects.[24] Finally, emission at the μs time-scale is observed in the energy-range commonly associated with the indirect excitonic emission band (1.5 eV–1.7 eV) and decays faster as crystal size decreases, as expected.

We use integrated photon counts from the μs decay for constructing the indirect emission spectra and the ps decay for the direct emission spectra. The emission decay at each energy was fitted with stretched exponentials in order to calculate the integrated photon count. Figure 5 shows the complete spectra with blue shifting indirect and red-shifting direct transition emissions obtained from the ps and the μs decays. The spectral dependence on Si-NCs size confirms

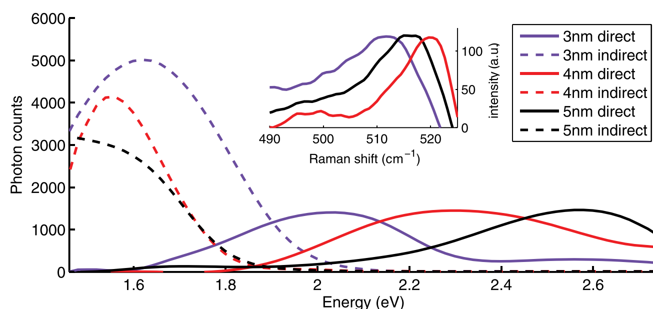

FIG. 5. Complete emission spectra measured for the integrated direct F-band and indirect S-band in films with different crystal sizes. The integrated emission is obtained at each energy from time-dependent PL. The inset shows Raman spectra with shifts from the bulk Si value of 521 cm^{-1}.

that the F-band is affected by quantum confinement. Room-temperature emission shows emission tuning from 810 to 708 nm (1.53 eV to 1.75 eV) for crystal diameters 5 nm to 3 nm. The Raman spectra (Fig. 5, inset) also confirm the existence of a broadened and red-shifted crystalline Si peak due to the increased separation of phonon modes. We can use this shift to confirm the average crystal sizes of 3, 4, and 5 nm, which is consistent with well-known PL emission energies in addition to estimates by the broadening of the Si (311) XRD peaks (Figure 2(b)).[25] Using the ratio of time-integrated ps-decay to the μs-decay, we calculate the relative efficiency of F-band emission. Fast emission occurs at a lower energy and is more efficient for smaller crystals (Fig. 4). The best relative efficiency we obtained was 5.2×10^{-4} for 3 nm crystals at 2.1 eV, a value comparable to that obtained by de Boer *et al.* ($\sim 10^{-3}$) confirming that our material is of high quality.

Hence, the time-resolved studies confirm that the electronic structure we measured by PDS is responsible for the emission characteristics of Si-NCs. F-band emission is consistent with direct recombination of electrons located in states red-shifted from the bulk Si Γ-point energy due to quantum confinement effects. F-band emission is unambiguously associated with high order heavy electron and mixed electron-electron and electron-hole states. It must be noted that the red-shifted emitting Γ-point states do not form a valley and cannot accumulate electrons. Thus, the emission must be metastable, as supported by the broad emission range shown in Figure 5 and the ultrafast sub-ns decay times.

V. CONCLUSION

While the path towards a Si-NC laser remains difficult, F-band emission may provide a new possible route. For strong light matter coupling in nano-cavities, the emitter homogeneous line-width must be much narrower than the cavity resonance. This requirement poses an inherent problem for the indirect transition in Si. Individual Si-NCs have a phonon-induced broadening of the emission line-width of 120 meV at room temperature, which can be reduced to 10 meV only by cooling at liquid nitrogen temperatures. The indirect emission, however, is strongly suppressed at low temperatures. In contrast, at low temperatures the Γ to Δ electron transfer rate will decrease and thus improve the direct transition efficiency. Hence, the ps decay may potentially offer a path to observing large Purcell enhancements in Si-NCs. Furthermore, the FCA loss that fundamentally limits the feasibility of a Si-NC laser at long wavelengths is strongly reduced at the shorter wavelengths where the direct transition is more efficient.

In conclusion, we show a direct experimental measurement of the effect of quantum confinement on the above-edge band structure of Si-NCs in an oxide matrix. We offer an experimental proof of the splitting of the Γ valley DOS, due to the opposite signs of the electron effective mass. The combination of absorption and emission provides a complete picture of the effect of quantum confinement on the electronic structure of Si-NCs and allows to resolve controversies in theoretical models. Our measurements are more consistent with Luttinger–Kohn model for a spherical

[This article is copyrighted as indicated in the article. Reuse of AIP content is subject to the terms at: http://scitation.aip.org/termsconditions. Downloaded to] IP: 171.67.216.22 On: Mon, 17 Mar 2014 23:00:43

geometry, showing that the pseudo-potential calculations and others under-predict the shifts of the energy levels.[17] The increase in emission efficiency of the direct transition with decreasing Si-NC size offers new opportunities for the use of silicon as a photonic material.

ACKNOWLEDGMENTS

W.M. prepared the samples and performed absorption measurements, A.M. designed and aided time resolved luminescence measurements. J.V. and A.S. supervised and directed the research. W.M. prepared the manuscript. All authors were involved in the discussion of results and editing of the manuscript.

W.M. gratefully acknowledges support from Office of Technology Licensing Stanford Graduate Fellowship. A.M. and J.V. acknowledge support from AFOSR MURI for Complex and Robust On-Chip Nanophotonics (Dr. Gernot Pomrenke), Grant No. FA9550-09-1-0704. A.S. gratefully acknowledges the Stanford Center for Integrated Systems and Electro Scientific Industries for financial support. We declare no competing financial interests.

[1]L. Pavesi, L. Dal Negro, C. Mazzoleni, G. Franzo, and F. Priolo, "Optical gain in silicon nanocrystals," Nature **408**, 440–444 (2000).
[2]L. T. Canham, "Silicon quantum wire array fabrication by electrochemical and chemical dissolution of wafers," Appl. Phys. Lett. **57**, 1046–1048 (1990).
[3]L. Dal Negro, M. Cazzanelli, L. Pavesi, S. Ossicini, D. Pacifici, G. Franzò, F. Priolo, and F. Iacona, "Dynamics of stimulated emission in silicon nanocrystals," Appl. Phys. Lett. **82**, 4636–4638 (2003).
[4]F. Iacona, C. Bongiorno, C. Spinella, S. Boninelli, and F. Priolo, "Formation and evolution of luminescent Si nanoclusters produced by thermal annealing of SiO[sub x] films," J. Appl. Phys. **95**, 3723–3732 (2004).
[5]V. A. Belyakov, V. A. Burdov, R. Lockwood, and A. Meldrum, "Silicon nanocrystals: Fundamental theory and implications for stimulated emission," Adv. Opt. Technol. **2008**, 279502.
[6]A. Polman and R. G. Elliman, "Optical gain from silicon nanocrystals—A critical perspective," in *Towards the First Silicon Laser*, edited by L. Pavesi *et al*. (Kluwer Academic Publishers, 2003), pp. 209–222.
[7]R. D. Kekatpure and M. L. Brongersma, "Fundamental photophysics and optical loss processes in Si-nanocrystal-doped microdisk resonators," Phys. Rev. A **78**, 023829 (2008).
[8]R. D. Kekatpure and M. L. Brongersma, "Quantification of free-carrier absorption in silicon nanocrystals with an optical microcavity," Nano Lett. **8**, 3787–3793 (2008).
[9]L. Tsybeskov, Ju. V. Vandyshev, and P. M. Fauchet, "Blue emission in porous silicon: Oxygen-related photoluminescence," Phys. Rev. B **49**, 7821(R) (1994).
[10]K. Luterová, I. Mikulskas, R. Tomasiunas, D. Muller, J.-J. Grob, J.-L. Rehspringer, and B. Hönerlage, "Stimulated emission in blue-emitting Si-implanted SiO2 films," J. Appl. Phys. **91**, 2896–2900 (2002).
[11]J. D. Holmes *et al*., "Highly luminescent silicon nanocrystals with discrete optical transitions," J. Am. Chem. Soc. **123**, 3743–3748 (2001).
[12]G. Allan and C. Delerue, "Fast relaxation of hot carriers by impact ionization in semiconductor nanocrystals: Role of defects," Phys. Rev. B **79**, 195324 (2009).
[13]F. Trojánek, K. Neudert, M. Bittner, and P. Malý, "Picosecond photoluminescence and transient absorption in silicon nanocrystals," Phys. Rev. B **72**, 075365 (2005).
[14]M. V. R. Krishna and R. A. Friesner, "Prediction of anomalous redshift in semiconductor clusters," J. Chem. Phys. **96**, 873–877 (1992).
[15]A. J. Williamson, J. C. Grossman, R. Hood, A. Puzder, and G. Galli, "Quantum Monte Carlo calculations of nanostructure optical gaps: Application to silicon quantum dots," Phys. Rev. Lett. **89**, 196803 (2002).
[16]F. Trani, G. Cantele, D. Ninno, and G. Iadonisi, "Tight-binding calculation of the optical absorption cross section of spherical and ellipsoidal silicon nanocrystals," Phys. Rev. B **72**, 075423 (2005).
[17]V. Vinciguerra, G. Franzo, F. Priolo, F. Iacona, and C. Spinella, "Quantum confinement and recombination dynamics in silicon nanocrystals embedded in Si/SiO[sub 2] superlattices," J. Appl. Phys. **87**, 8165–8173 (2000).
[18]W. B. Jackson, N. M. Amer, A. C. Boccara, and D. Fournier, "Photothermal deflection spectroscopy and detection," Appl. Opt. **20**, 1333–1344 (1981).
[19]D. Timmerman and T. Gregorkiewicz, "Power-dependent spectral shift of photoluminescence from ensembles of nanocrystals," Nanoscale Res. Lett. **7**, 389 (2012).
[20]C. Garcia, B. Garrido, P. Pellegrino, R. Ferre, J. A. Moreno, J. R. Morante, L. Pavesi, and M. Cazzanelli, "Size dependence of lifetime and absorption cross section of Si nanocrystals embedded in SiO_2," Appl. Phys. Lett. **82**, 1595–1597 (2003).
[21]A. A. Prokofieva, A. S. Moskalenko, I. N. Yassievicha, W. D. A. M. de Boer, D. Timmerman, H. Zhang, W. J. Buma, and T. Gregorkiewicz, "Direct bandgap optical transitions in Si nanocrystals," JETP Lett. **90**(12), 758–762 (2009).
[22]W. D. A. M. de Boer, D. Timmerman, K. Dohnalová, I. N. Yassievich, H. Zhang, W. J. Buma, and T. Gregorkiewicz, "Red spectral shift and enhanced quantum efficiency in phonon-free photoluminescence from silicon nanocrystals," Nat. Nanotechnol. **5**, 878–884 (2010).
[23]V. I. Klimov, Ch. J. Schwarz, D. W. McBranch, and C. W. White, "Initial carrier relaxation dynamics in ion-implanted Si nanocrystals: Femtosecond transient absorption study," Appl. Phys. Lett. **73**, 2603–2605 (1998).
[24]A. Tewary, R. D. Kekatpure, and M. L. Brongersma, "Controlling defect and Si nanoparticle luminescence from silicon oxynitride films with CO2 laser annealing," Appl. Phys. Lett. **88**, 093114–093114-3 (2006).
[25]H. Xia, Y. L. He, L. C. Wang, W. Zhang, X. N. Liu, X. K. Zhang, D. Feng, and H. E. Jackson, "Phonon mode study of Si nanocrystals using micro-Raman spectroscopy," J. Appl. Phys. **78**, 6705–6708 (1995).

[This article is copyrighted as indicated in the article. Reuse of AIP content is subject to the terms at: http://scitation.aip.org/termsconditions. Downloaded to] IP: 171.67.216.22 On: Mon, 17 Mar 2014 23:00:43